Actin alpha 2, smooth muscle, a transforming growth factor-β1-induced factor, regulates collagen production in human periodontal ligament cells via Smad2/3 pathway

ファカタバ, ナーティ

ARTICLE IN PRESS
+ MODEL
Journal of Dental Sciences xxx (xxxx) xxx

Available online at www.sciencedirect.com
ScienceDirect
journal homepage: www.e-jds.com

Original Article

Actin alpha 2, smooth muscle, a transforming growth factor-β1-induced factor, regulates collagen production in human periodontal ligament cells via Smad2/3 pathway

Naati Fakatava [a], Hiromi Mitarai [b*], Asuka Yuda [b], Akira Haraguchi [b], Hiroko Wada [c], Daigaku Hasegawa [d], Hidefumi Maeda [e], Naohisa Wada [a]

[a] *Department of General Dentistry, Division of Interdisciplinary Dentistry, Faculty of Dental Science, Kyushu University, Fukuoka, Japan*
[b] *Division of General Dentistry, Kyushu University Hospital, Kyushu University, Fukuoka, Japan*
[c] *Laboratory of Oral Pathology, Faculty of Dental Science, Kyushu University, Fukuoka, Japan*
[d] *Department of Endodontology, Kyushu University Hospital, Kyushu University, Fukuoka, Japan*
[e] *Department of Endodontology and Operative Dentistry, Division of Oral Rehabilitation, Faculty of Dental Science, Kyushu University, Fukuoka, Japan*

Received 19 July 2022; Final revision received 26 August 2022
Available online ■ ■ ■

KEYWORDS
ACTA2;
Collagen production;
Periodontal ligament;
Smad2/3;
TGF-β1

Background/purpose: Actin alpha 2, smooth muscle (ACTA2) is an actin isoform that forms the cytoskeleton. Actin plays a crucial role in numerous cellular functions. ACTA2 is a marker of functional periodontal ligament (PDL) fibroblasts and is upregulated by transforming growth factor-β1 (TGF-β1); however, the underlying function of ACTA2 in PDL tissue is unknown. We aimed to examine the localization and potential function of ACTA2 in PDL tissues and cells.
Materials and methods: RNA expression was determined using semi-quantitative reverse transcription—polymerase chain reaction (RT-PCR) and quantitative RT-PCR. Protein expression was determined using immunofluorescence staining and Western blot analysis. Soluble and insoluble collagen production was examined using the Sircol collagen assay and picrosirius

Abbreviations: ACTA2, Actin alpha2, smooth muscle; TGF-β1, transforming growth factor-β1; PDL, periodontal ligament; COLIA1, collagen typeIalpha1 chain; POSTN, periostin; FBNI, fibrillin-I.

* Corresponding author. Division of General Dentistry, Kyushu University Hospital, Kyushu University, 3-1-1 Maidashi, Higashi-ku, Fukuoka 812-8582, Japan.
E-mail address: mitarai@dent.kyushu-u.ac.jp (H. Mitarai).

https://doi.org/10.1016/j.jds.2022.08.030

Please cite this article as: N. Fakatava, H. Mitarai, A. Yuda et al., Actin alpha 2, smooth muscle, a transforming growth factor-β1-induced factor, regulates collagen production in human periodontal ligament cells via Smad2/3 pathway, Journal of Dental Sciences, https://doi.org/10.1016/j.jds.2022.08.030

red staining, respectively. Small interfering RNA (siRNA) was used for knockdown assay to examine the effect of ACTA2 in human PDL cells.
Results: ACTA2 expression was observed in human primary PDL cells and PDL cell line (2—23 cells). TGF-β1 upregulated ACTA2, *collagen type I alpha1 chain* (*COL1A1*), *periostin* (*POSTN*), and *fibrillin-I*(*FBN1*) expression and soluble and insoluble collagen production in 2—23 cells. However, ACTA2 depletion by siRNA strongly suppressed PDL-related gene expression and collagen production compared with those of TGF-β1—stimulated control cells. Furthermore, ACTA2 knockdown significantly suppressed the phosphorylation of Smad2 and Smad3.
Conclusion: ACTA2 plays a crucial role in PDL-related marker expression and collagen production via Smad2/3 phosphorylation. Our findings might contribute to the development of novel and effective periodontal therapies.

Introduction

The periodontal ligament (PDL) is a collagen-rich fibrous connective tissue firmly anchored between the alveolar bone and root cementum. Various approaches have been employed to establish a PDL regeneration therapy which ensures that PDL tissue is maintained without mineralization, despite the fact that the PDL connects the alveolar bone and cementum, two specialized mineralized tissues. Therefore, investigating and understanding the functions of genes strongly expressed in the PDL is required.

The cytoskeleton organizes the cell content and is crucial for cell functioning. It connects the cell and its external environment and generates forces that enable the cell to move and change its size and shape.[1] Actin alpha 2, smooth muscle (ACTA2), also known as alpha smooth muscle actin (α-SMA), is one of six actin isoforms that form the cytoskeleton and is predominantly found in smooth muscle cells.[2] ACTA2 plays a crucial role in cell focal adhesion, migration, transcriptional and shape regulations, and contractile activity.[3—6] ACTA2 is also expressed in human PDL cells.[7,8] Therefore, we assumed that cytoskeletal structure, ACTA2, might affect cellular activities in PDL cells; however, its function has not yet been elucidated.

TGF-β1 is a multifunctional cytokine expressed in PDL tissues and is related to numerous cellular processes, including differentiation, extracellular matrix protein production, wound healing, proliferation, migration, apoptosis, and angiogenesis.[9—13] TGF-β1 intracellular signaling is mediated by Smads, the main signal transducers of TGF-β1 receptors. In the canonical TGF-β—Smad signaling pathway, Smad2/3 phosphorylation is required to activate or repress the transcription of several genes.[14—16] TGF-β1 is expressed in mouse PDL tissue, according to immunohistochemical findings, and it induces ACTA2 expression in human PDL cells.[8] We have previously reported that mechanical stress upregulates TGF-β1 expression and induces collagen production.[17] Thus, ACTA2 might be involved in TGF-β1—related collagen production; however, its function remains unclear.

We hypothesized that ACTA2 played a crucial role in PDL tissue homeostasis. Therefore, in this study, we examined whether ACTA2 was involved in the effects of TGF-β1 on collagen production in human PDL cells.

Materials and methods

Cell culture

Two human PDL cell (HPDLC) populations were isolated from healthy premolars of a 23-year-old male (HPDLC-3S) and a 29-year-old female (HPDLC-5Y) with informed consent, as described previously.[18] The cells (passages 4—6) were grown as monolayers in 10 cm dishes. A clonal cell line 2—23 (2—23 cells) was established previously.[19] The cells used in all experiments were maintained in alpha minimum essential medium (α-MEM; Gibco-BRL, Grand Island, NY, USA) containing 10% fetal bovine serum (FBS; 10% FBS/α-MEM; Sigma—Aldrich, St Louis, MO, USA) at 37 °C in a humidified atmosphere of 5% CO2 and 95% air. All procedures were performed in compliance with the requirements of the Institutional Review Board for Human Genome/Gene Research (approval number: 30—167) and the Research Ethics Committee (approval number: 27—76) of Kyushu University.

Reagents

Recombinant human TGF-β1 (rhTGF-β1, 240-b-002) was purchased from R&D Systems (Minneapolis, MN, USA).

Quantitative real-time reverse transcription—polymerase chain reaction (RT-PCR) and semi-quantitative RT-PCR

Quantitative RT-PCR and semi-quantitative RT-PCR were performed as described previously.[17] Primer sequences, annealing temperatures, cycle number, and product sizes are shown in Tables 1 and 2.

Table 1 Quantitative RT-PCR primer sequences, annealing temperatures, cycle numbers, and product sizes. ACTA2: *Actin alpha 2*, smooth muscle, COL1A1: *collagen type I alpha1 chain*, POSTN: *periostin*, FBN1: *fibrillin-I*, and GAPDH: *glyceraldehyde-3-phosphate dehydrogenase*.

Gene	Primer sequence forward (5′—3′)/reverse (3′—5)	Cycles	Annealing temperature (°C)	Amplicon (bp)
ACTA2	CAATGAGCTTCGTGTTGCCC/GGCATAGAGAGACAGCACCG	40	60	160
β-Actin	ATTGCCGACAGGATGCAGA/GAGTACTTGCGCTCAGGAGGA	40	60	89
COL1A1	AATGTGGTTCGTGACCGTGA/AGCCTTGGTTGGGGTCAATC	40	60	181
FBN1	TGCACCTATGGAACCATGTGATAGA/AAGTGATCCACTGTGTGCCAACTC	40	60	190
γ-Actin	CAATGAGCGGTTCCGGTGTC/CTCCTTCTGCATCCTGTCGG	40	60	196
POSTN	CACAACCTGGAGACTGGACA/TGCTTCCTTGTGTGGTCTTT	40	60	198
GAPDH	GTCAGTGGTGGACCTGACC/TGCTGTAGCCAAATTCGTTG	40	60	245

Table 2 Semi-quantitative RT-PCR primer sequences, annealing temperatures, cycle numbers, and product sizes.

Gene	Primer sequence forward (5′—3′)/reverse (3′—5′)	Cycles	Annealing temperature (°C)	Amplicon (bp)
ACTA2	GACGATGCTCCCAGGGCTG/GAGAGACAGCACCGCCTGG	27	61	367
GAPDH	TCCACCACCCTGTTGCTGTA/ACCACAGTCCATGCCATCCAC	20	59	452

Small interfering RNA (siRNA) transfection

We purchased siRNAs for ACTA2 (Mission siRNA; SASI_Hs01_00097,021) and scramble control (Mission siRNA Universal Negative Control no2; SIC-002-10) from Sigma-—Aldrich. The effects of ACTA2 knockdown by siRNA were analyzed as previously described.[20]

Picrosirius red staining

2-23 cells (2×10^4 cells/well) were cultured in 24-well plates with 2% FBS/α-MEM with or without rhTGF-β1 (10 ng/mL) for 5 days. Fibrillar collagen formed by 2—23 cells was detected as previously described.[17]

Sircol collagen assay

Sircol collagen assay (Biocolor Ltd, Belfast, UK) was used to assess the total soluble collagen produced in the cell supernatant. 2—23 cells (4×10^4 cells/well) were cultured in culture medium with or without rhTGF-β1 (10 ng/mL) for 5 days. The cell supernatants were collected and analyzed as previously described.[17]

Western blot analysis

The protein expression levels were determined according to the issued procedures. The membrane was incubated with the following primary antibodies: mouse monoclonal anti-GAPDH (dilution, 1:5000; SC-47724; Santa Cruz Biotechnology, Santa Cruz, CA, USA), mouse monoclonal anti-ACTA2 (dilution, 1:2000; ab7817; Abcam, Cambridge, UK), rabbit monoclonal anti-Smad2 (dilution, 1:1000; #5339; Cell Signaling Technology, Danvers, MA, USA), rabbit monoclonal phospho-Smad2 (Ser465/467; dilution, 1:1000; #3108; Cell Signaling Technology), rabbit monoclonal anti-Smad3 (dilution, 1:1000; #9523; Cell Signaling Technology), and rabbit monoclonal anti-Smad3 (phospho-S423 + S425; dilution, 1:1000; ab52903; Abcam). Thereafter, the membrane was incubated with secondary anti-mouse IgG (dilution, 1:1000; R&D Systems) or anti-rabbit IgG (dilution, 1:1000; R&D Systems). After the membrane was washed thoroughly, the reactive bands were visualized using the ECL Select western blotting Detection System (GE Healthcare, Buckinghamshire, UK).

Immunocytofluorescence staining

Briefly, 2—23 cells were fixed in 10% PFA neutral buffer (NACALAI TESQUE, Inc. Kyoto, Japan) for 15 min at room temperature and then permeabilized with methanol (Wako, Osaka, Japan) at −20 °C for 10 min. After blocking with 2% bovine serum albumin (NACALAI TESQUE, Inc) in PBS for 1 h at room temperature, the cells were incubated with mouse monoclonal anti-ACTA2 (dilution, 1:100; Abcam; ab7817) and then washed with PBS. Thereafter, the cells were incubated with Alexa Fluor 488-conjugated donkey anti-mouse antibody (dilution, 1:100; Thermo Fisher Scientific, Waltham, MA, USA) for 1 h at room temperature. To stain F-actin, cells were incubated with Alexa Fluor™ 488 phalloidin (Thermo Fisher Scientific) in PBS (dilution, 1:20) for 30 min at room temperature. The cells were then washed with PBS, and the nuclei were counterstained with Fluoro-KEEPER Antifade Reagent Non-Hardening Type with 4′,6-diamidino-2-phenylindole (DAPI) (NACALAI TESQUE, Inc). The cells were imaged and analyzed using an all-in-one fluorescence microscope BZ-X100 (Keyence Corporation, Osaka, Japan).

Cell proliferation assay

2-23 cells (5×10^3 cells/well) were cultured in a 48-well plates (Becton Dickinson Labware, Lincoln Park, NJ) in 250 μl of 10% FBS/α-MEM. At 1, 2, and 3 days, the proliferation rate was measured using a Premix WST-1 Cell Proliferation Assay System (Takara Bio Inc, Shiga, Japan) according to the manufacturer's instructions. Briefly, at the indicated time points, 25 μl of the kit reagent WST-1 was added to the culture medium of each well. After 1 h, 100 μl of supernatant was collected from each well and the absorbance was

measured at 450 nm using a microplate reader (Infinite F50; Tecan Group Ltd., Männedorf, Switzerland).

Cell migration assay

2—23 cells (3 × 10^5 cells/well) were seeded on 12-well plates (Becton Dickinson Labware), and allowed to incubate for 24 h. Then a scratch-wound was made across the diameter of the well using the end of a 200 μl pipette tip, and scraped cells or cell fragments were removed by washing three times with PBS. The cells were maintained in culture medium. For each well, images were taken at 0 and 10 h after the scratch-wound, the cellular migration area was visualized using a microscope (DMIRB; Leica, Wetzlar, Germany) at a magnification of 10× and quantified by Image J software (NIH, Bethesda, MD, USA).

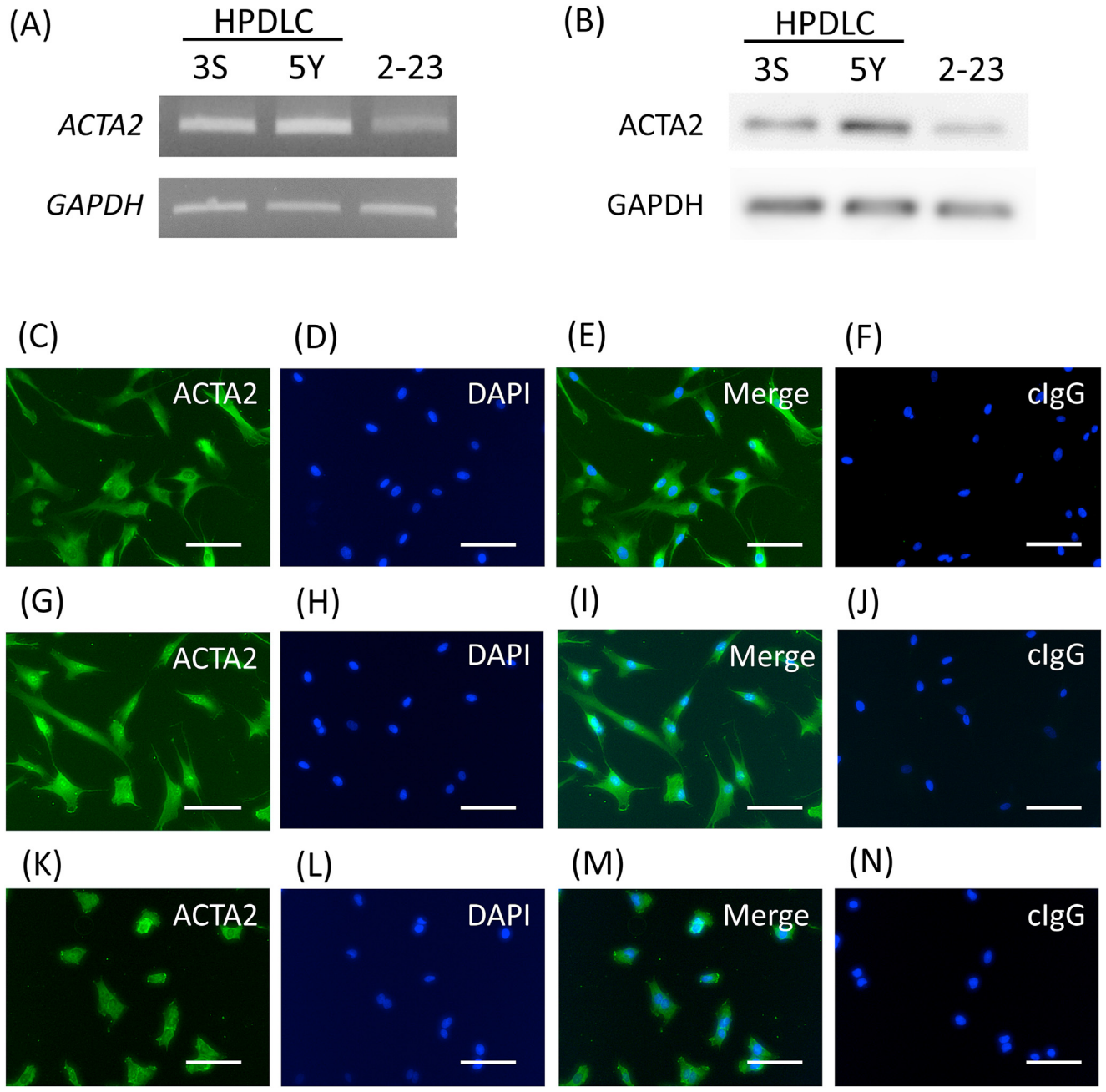

Figure 1 ACTA2 expression in 2—23 cells. (A) *ACTA2* mRNA expression in HPDLC-3S, HPDLC-5Y, and 2—23 cells was assessed using semi-quantitative RT-PCR. (B) ACTA2 expression in HPDLC-3S, HPDLC-5Y, and 2—23 cells was determined using Western blot analysis. GAPDH was used as a loading control in (A) and (B). (C—N) ACTA2 expression in HPDLC-3S, HPDLC-5Y, and 2—23 cells was evaluated using immunofluorescence staining. (C, G, K) HPDLC-3S, HPDLC-5Y, and 2—23 cells were fixed and incubated with ACTA2 antibody (green). (D, H, L) Nuclei were stained with DAPI (blue). Two-color merged images are shown in (E, I, M). (F, J, N) HPDLC-3S, HPDLC-5Y, and 2—23 cells were fixed and incubated with control mouse IgG. Nuclei were stained with DAPI (blue). Scale bars represent 100 μm cIgG, control immunoglobulin.

Statistical analysis

All experiments were performed in quadruplicate, and all values are expressed as the mean ± standard deviation (SD). Statistically significant differences between paired observations were analyzed using non-parametric analysis followed by Mann—Whitney U test. Statistically significant differences between groups were analyzed using one-way analysis of variance (ANOVA) followed by Tukey's multiple comparison test. Those tests were done with GraphPad Prism version 9 for Windows (GraphPad Software, San Diego, CA, USA). $^{*}*P < 0.01$, $*P < 0.05$, $***P < 0.001$, and $****P < 0.0001$ were considered statistically significant.

Results

ACTA2 expression in human PDL cells

To analyze ACTA2 expression and function in human PDL cells, we used previously established 2—23 cells with typical PDL characteristics.[19,20] Semi-quantitative PCR analysis demonstrated that 2—23 cells expressed *ACTA2* mRNA, similarly to HPDLC-3S and 5Y (Fig. 1A). In addition, Western blot analysis revealed that HPDLC-3S, 5Y, and 2—23 cells expressed ACTA2 (Fig. 1B). Immunocytofluorescence analysis revealed positive staining for ACTA2 in the cytoplasm of HPDLC-3S (Fig. 1C—E), 5Y (Fig. 1G—I), and 2—23 cells (Fig. 1K—M). Control staining with normal rabbit IgG was negative for all three cells (Fig. 1F, J, N).

Effects of TGF-β1 on ACTA2 and PDL-related gene expression and collagen production in a human PDL cell line

To assess the effects of TGF-β1 stimulation on the morphology and expression of PDL-related genes in a human PDL cell line, we cultured 2—23 cells with or without rhTGF-β1 (10 ng/mL). Previous studies have shown that TGF-β1 stimulate actin stress fiber formation and regulate the cytoskeletal reorganization and morphology.[21] Therefore, the present study investigated the effect of TGF-β1 on the morphology in 2—23 cells. 2—23 cells stimulated with TGF-β1 showed potent actin cytoskeleton reorganization by the formation of stress fibers in comparison to 2—23 cells without TGF-β1 stimulation, which was detected with Alexa Fluor™ 488 phalloidin (Fig. 2A and B). Quantitative RT-PCR demonstrated that the expression of *ACTA2* (Fig. 2C) and other PDL-related genes, including *COL1A1* (Fig. 2D), *POSTN* (Fig. 2E), and *FBN1* (Fig. 2F) were significantly upregulated in 2—23 cells cultured with rhTGF-β1 for 24 h compared with that in untreated control cells. A Sircol collagen assay demonstrated that the amount of soluble collagen was

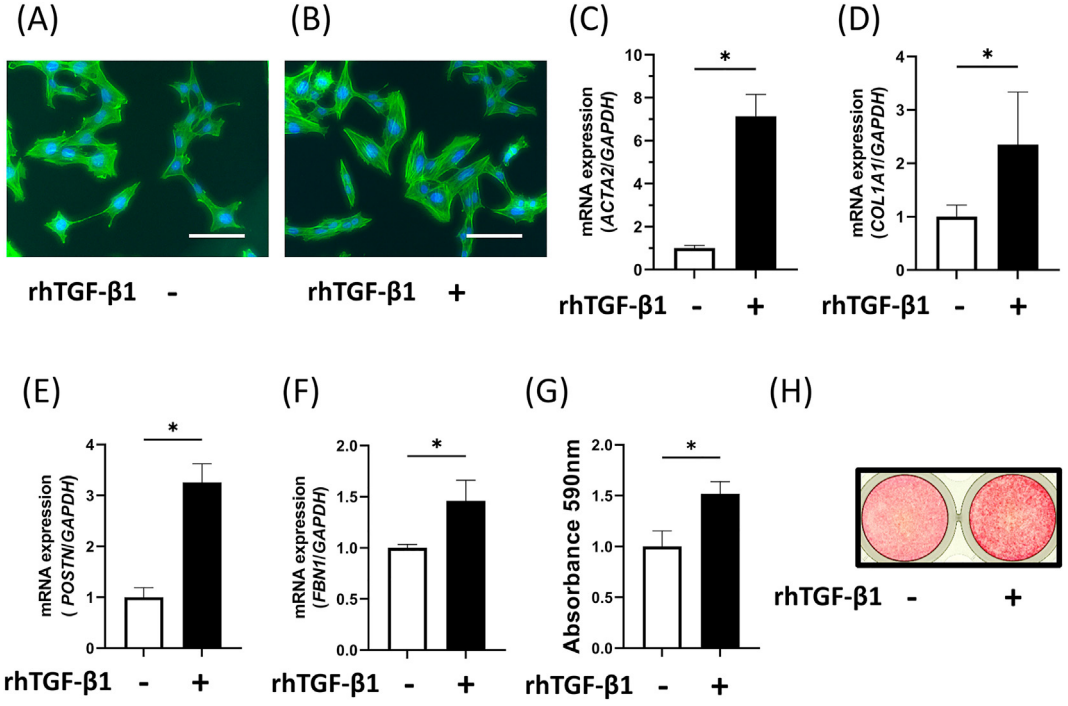

Figure 2 Effects of TGF-β1 on *ACTA2* and PDL-related gene expression and collagen production in 2—23 cells. (A and B) Phalloidin staining (green) of filamentous actin was performed to analyze the cell shape of 2—23 cells with or without TGF-β1 for 24 h. Nuclei were stained with DAPI (blue). (A) 2—23 cells cultured without TGF-β1. (B) 2—23 cells cultured with TGF-β1. Scale bars represent 100 μm. (C—F) Quantitative RT-PCR was performed to analyze the expression of *ACTA2* (C) and PDL-related genes, including *COL1A1* (D), *POSTN* (E), and *FBN1* (F) in 2—23 cells cultured in 2% FBS/α-MEM with or without rhTGF-β1 (10 ng/mL) for 24 h. (G) Sircol collagen assay for quantification of soluble collagen in the supernatants of 2—23 cells cultured in 2% FBS/α-MEM with or without rhTGF-β1 (10 ng/mL) for 5 days. (H) Picrosirius red staining of 2—23 cells cultured in 2% FBS/α-MEM with or without rhTGF-β1 (10 ng/mL) for 5 days. Statistical analysis was performed using non-parametric analysis followed by Mann—Whitney U test. All values are expressed as means ± SD (error bars) of four independent experiments. $*P < 0.05$.

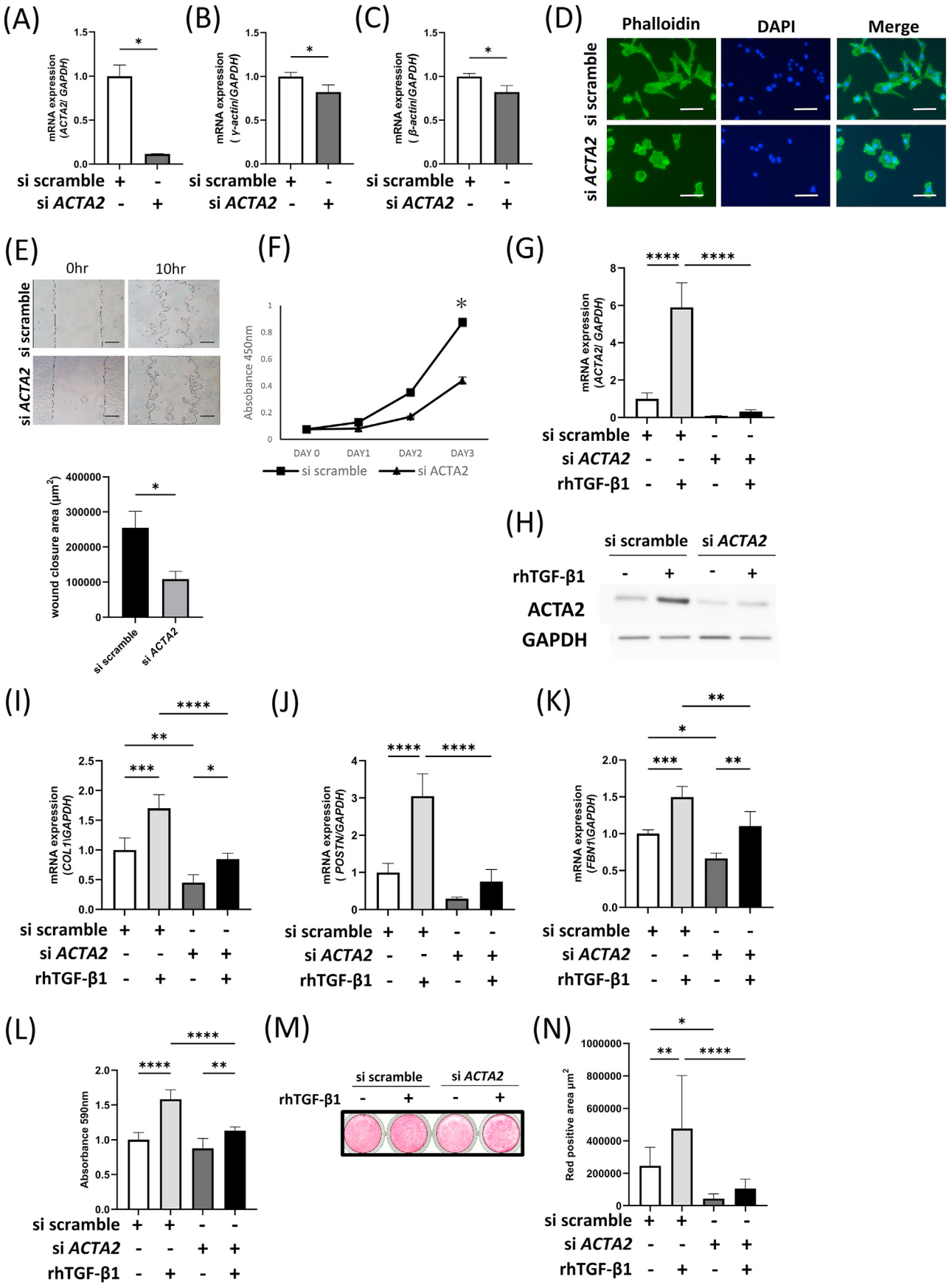
(A)
mRNA expression (ACTA2/ GAPDH)
si scramble + -
si ACTA2 - +
(B)
mRNA expression (γ-actin/GAPDH)
si scramble + -
si ACTA2 - +
(C)
mRNA expression (β-actin/GAPDH)
si scramble + -
si ACTA2 - +
(D)
Phalloidin
DAPI
Merge
si scramble
si ACTA2
(E)
0hr
10hr
si scramble
si ACTA2
wound closure area (μm²)
si scramble
si ACTA2
(F)
Absobance 450nm
DAY 0
DAY1
DAY2
DAY3
si scramble
si ACTA2
(G)
mRNA expression (ACTA2/ GAPDH)
si scramble + + - -
si ACTA2 - - + +
rhTGF-β1 - + - +
(H)
si scramble
si ACTA2
rhTGF-β1 - + - +
ACTA2
GAPDH
(I)
mRNA expression (COL1/GAPDH)
si scramble + + - -
si ACTA2 - - + +
rhTGF-β1 - + - +
(J)
mRNA expression (POSTN/GAPDH)
si scramble + + - -
si ACTA2 - - + +
rhTGF-β1 - + - +
(K)
mRNA expression (FBN1/GAPDH)
si scramble + + - -
si ACTA2 - - + +
rhTGF-β1 - + - +
(L)
Absorbance 590nm
si scramble + + - -
si ACTA2 - - + +
rhTGF-β1 - + - +
(M)
si scramble
si ACTA2
rhTGF-β1 - + - +
(N)
Red positive area μm²
si scramble + + - -
si ACTA2 - - + +
rhTGF-β1 - + - +

significantly higher in the supernatants of 2–23 cells cultured with rhTGF-β1 for 5 days (Fig. 2G). In addition, 2–23 cells treated with rhTGF-β1 for 5 days showed increased picrosirius red-positive areas, which represent fibrillary collagen formation (Fig. 2H).

Effects of ACTA2 knockdown on TGF-β1–stimulated human PDL cell function

We examined the effect of ACTA2 knockdown by siRNA transfection. Quantitative RT-PCR confirmed that *ACTA2* mRNA expression in 2–23 cells treated with *ACTA2* siRNA for 48 h was significantly reduced compared with scramble siRNA (mean ± stdev: 9.2% ± 0.7516, $P = 0.0013$) (Fig. 3A). We also examined the expression of β- and γ-actin to confirm the *ACTA2* siRNA effect on other actin isoforms. The mRNA expression level of β-actin was 82.02% ± 8.286 (mean ± std. dev., $P = 0.0049$), and γ-actin was 82.05% ± 8.286 (mean ± std. dev., $P = 0.0013$) in 2–23 cells treated with *ACTA2* siRNA compared with scramble siRNA, respectively (Fig. 3B and C), *ACTA2* siRNA showed not so much effect on the mRNA expression of other actin isoforms compared with the effect on ACTA2 mRNA expression. We next stained the cells for F-actin to observe the cell shape change of 2–23 cells. 2–23 cells treated with scramble siRNA exhibited a fibroblast-like morphology with a spindle-shaped cell form, while 2–23 cells treated with *ACTA2* siRNA showed round appearance (Fig. 3D). To assess the effect of ACTA2 on migration of 2–23 cells, we examined scratch wound healing assay. The area of migrated cells was significantly smaller in *ACTA2* siRNA transfected-2-23 cells for 10 h than in the scramble siRNA transfected-2-23 cells (Fig. 3E). In addition, we examined WST-1 assay to assess the effect of ACTA2 on proliferation of 2–23 cells. Proliferation rate of *ACTA2* siRNA transfected-2-23 cells was significantly downregulated at 3 days compared with scramble siRNA transfected-2-23 cells (Fig. 3F). We next examined the effect of ACTA2 knockdown by *ACTA2* siRNA on TGF-β1–induced PDL-related gene expression and collagen production in 2–23 cells. Quantitative RT-PCR and Western blot analysis confirmed that the expression of *ACTA2* mRNA and ACTA2 in 2–23 cells was upregulated by TGF-β1 but downregulated by *ACTA2* siRNA in the presence of TGF-β1 (Fig. 3G and H). Moreover, *COL1A1* (Fig. 3I), *POSTN* (Fig. 3J), and *FBN1* (Fig. 3K) mRNA expression was significantly downregulated in *ACTA2* siRNA-treated 2–23 cells in the presence of TGF-β1 compared with that in scramble siRNA-treated cells in the presence of TGF-β1. In addition, the amount of soluble and fibrillar collagen produced by 2–23 cells treated with TGF-β1 for 5 days was significantly decreased by *ACTA2* siRNA treatment (Fig. 3L–N).

Effects of ACTA2 knockdown on TGF-β1-induced phosphorylation and nuclear localization of Smad2 and Smad3 in a human PDL cell line

We examined the effects of ACTA2 knockdown on the phosphorylation of Smad2 and Smad3 in 2–23 cells. From the time course of Smad2/3 activation following TGF-β1 exposure, we observed Smad2/3 phosphorylation from the 15 min time point of TGF-β1 treatment (Fig. 4A). Intriguingly, in the presence of *ACTA2* siRNA, the phosphorylation of Smad2 and Smad3 was significantly downregulated after 15 min of TGF-β1 stimulation compared with that in the presence of scramble siRNA (Fig. 4B–E). These results indicated that ACTA2 affected TGF-β1–signaling activities in PDL cells.

Discussion

ACTA2 is expressed in numerous tissues and supports cytoskeletal dynamics,[22] cell motility and contractility. PDL tissue is constantly exposed to forces during the mechanical stress of occlusion and mastication, and ACTA2 is expressed in post-emergent tooth eruption, predominantly in adult

Figure 3 Effects of ACTA2 knockdown on TGF-β1–induced PDL-related gene expression and collagen production in 2–23 cells. (A–C) Quantitative RT-PCR was performed to analyze *ACTA2* (A), β-actin (B), and γ-actin (C) mRNA expression in 2–23 cells transfected with *ACTA2* siRNA or universal negative control (scramble siRNA). (D) Phalloidin staining (green) of filamentous actin was performed to analyze the cell shape of 2–23 cells transfected with *ACTA2* siRNA or scramble siRNA for 48 h. Nuclei were stained with DAPI (blue). Scale bars represent 100 μm. (E) The effects of ACTA2 on migration of 2–23 cells were assessed with a scratch wound healing assay. The dashed lines delimit the initial wounded regions. At 10 h after wounding, the area that scramble or *ACTA2* siRNA transfected-2-23 cells migrated into the wound space were analyzed. Scale bars represent 200 μm. Statistically analysis was performed using non-parametric analysis followed by Mann–Whitney U test. All values are expressed as means ± SD (error bars) of four independent experiments. $^{*}P < 0.05$. (F) The effects of ACTA2 on proliferation of 2–23 cells were examined by WST-1 assay. Graphs show the time course of the increase in cell numbers of cells. Square dot, 2–23 cells transfected with scramble siRNA; triangle dot, 2–23 cells transfected with ACTA2 siRNA. Statistically analysis was performed using non-parametric analysis followed by Mann–Whitney U test. All values are expressed as means ± SD (error bars) of four independent experiments. $^{*}P < 0.05$. (G, H) Quantitative RT-PCR (G) and Western blot analysis (H) were performed to analyze the expression of *ACTA2* mRNA and ACTA2 in 2–23 cells treated with or without rhTGF-β1 (10 ng/mL) for 24 h in the presence of scramble siRNA or *ACTA2* siRNA. GAPDH was used as a loading control. (I–K) Quantitative RT-PCR was performed to analyze *COL1A1* (I), *POSTN* (J), and *FBN1* (K) mRNA expression in 2–23 cells treated with or without rhTGF-β1 (10 ng/mL) for 24 h in the presence of scramble siRNA or *ACTA2* siRNA. (L) Sircol collagen assay for quantification of soluble collagen in the supernatants of 2–23 cells treated with or without rhTGF-β1 (10 ng/mL) for 5 days in the presence of scramble siRNA or *ACTA2* siRNA. (M) Picrosirius red-positive areas were photographed and measured using a microscope. (N) Picrosirius red staining of 2–23 cells treated with or without rhTGF-β1 (10 ng/mL) for 5 days in the presence of scramble siRNA or *ACTA2* siRNA. Statistical analysis was performed using one-way ANOVA followed by Tukey's test. All values are expressed as means ± SD (error bars) of four independent experiment. $^{*}P < 0.05$, $^{**}P < 0.01$, $^{***}P < 0.001$, and $^{****}P < 0.0001$.

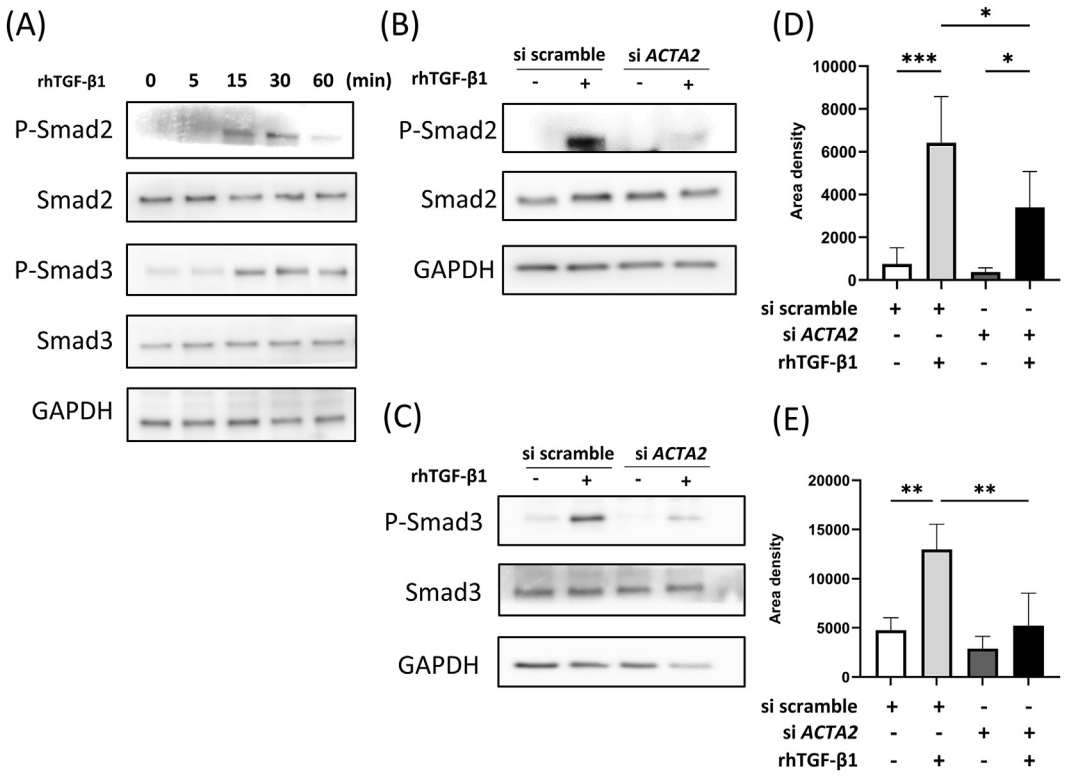

Figure 4 The effects of ACTA2 knockdown on the phosphorylation of Smad2 and Smad3 in 2—23 cells. (A) 2—23 cells were stimulated with rhTGF-β1 (10 ng/mL) for 0, 5, 15, 30, and 60 min. Western blot analysis was performed to detect phosphorylated (p)-Smad2 and p-Smad3 expression. (B—E) The effects of ACTA2 knockdown on the phosphorylation of Smad2 and Smad3 after TGF-β1 stimulation. 2—23 cells were cultured with or without rhTGF-β1 (10 ng/mL) in the presence of scramble siRNA or *ACTA2* siRNA for 15 min. Western blot analysis was performed to detect p-Smad2 (B) and p-Smad3 (C) expression. Phosphorylated Smad levels were compared with total Smad2 (B) or Smad3 (C) expression levels, and GAPDH was used as a loading control. (D and E) The integrated optical density of p-Smad2 (D) or p-Smad3 (E) bands was quantified using Image J software. The signal intensity of bands was normalized to that of GAPDH for statistical analysis. All values are expressed as means ± SD (error bars) of four independent experiment. Statistical analysis was performed using one-way ANOVA followed by Tukey's test. $^{*}P < 0.05$, $^{**}P < 0.01$, and $^{***}P < 0.001$.

mouse PDL tissues.[23] In our study, ACTA2 was predominantly detected in human PDL cells. Thus, ACTA2 might be an essential factor in PDL and, particularly, mature PDL cells and might play an important role in these cells.

TGF-β1 is predominantly expressed in PDL tissue and is a potent stimulator which may induce various fibroblastic differentiations of PDL cells.[8] Notably, in this study, PDL-related genes, including *COL1A1*, *POSTN*, *FBN1* and *ACTA2*, and collagen production were upregulated by TGF-β1. Since PDL-related genes contribute to maintaining PDL integrity; formation, tissue architecture, and normal cell alignment,[24,25] TGF-β1 signaling might influence PDL tissue remodeling.

In this study, loss of ACTA2, one of actin isoforms, in 2—23 cells led to cell shape change and suppressed proliferation potential and migration activity, suggesting ACTA2 in PDL cells could possess crucial roles in PDL cell cytoskeleton and function. In addition, loss of ACTA2 led to a significant downregulation of TGF-β1-stimulated collagen production, and the mRNA expression of other PDL-related markers, *POSTN* and *FBN1*. Collagen fiber regeneration is a homeostatic and wound healing response in PDL.[26,27] A previous study has demonstrated that TGF-β1 upregulates soluble and insoluble collagen production in adult rat cardiac ventricular fibroblasts,[28] which is consistent with our results. Taken together, these results indicated that ACTA2 regulated TGF-β1-induced remodeling of PDL tissue.

Actins are essential components of the cytoskeleton in mammalian cells, and actin dynamics are linked to gene transcription and interact with the nuclear genome.[29] The key finding of our study was that the phosphorylation of Smad2 and Smad3, canonical transcriptional factors of TGF-β1, was significantly downregulated after transduction with *ACTA2* siRNA compared with that after transduction with scramble siRNA, suggesting that ACTA2 was involved in the canonical TGF-β1 signaling pathway. However, the biological mechanism of involvement in the phosphorylation of Smad2 and Smad3 is still unclear. Previous studies have found that actin polymerization controls some signaling pathway,[30,31] and cytoskeletal alterations reduce collagen production via TGF-β1 in human dermal fibroblast cells.[32—34] ACTA2 knockdown may affect the actin polymerization and downregulate the phosphorylation of Smad2/3 in human periodontal ligament cells, but further studies are required.

In summary, ACTA2 was expressed in PDL tissues and a human PDL cell line. TGF-β1 enhanced the mRNA expression of *ACTA2* and other PDL-related genes and collagen production, and ACTA2 was involved in these processes by affecting TGF-β1—enhanced Smad2/3 phosphorylation. Further studies are required to clarify the detailed functional mechanism of ACTA2. Nevertheless, ACTA2 might be a critical factor in the homeostatic maintenance of PDL tissue. TGF-β1 known as multi-functional cytokine might induce both of expected and unexpected effects on cells and tissues, thus it could be difficult to control their balance when considering clinical applications. In order to focus on collagen production or maturation of PDL cell by inducing PDL related gene expression, delivering ACTA2 would be expected to exert limited effects. We therefore propose that ACTA2 may represent a potential therapeutic approach to regenerate PDL tissue.

Declaration of competing interest

The authors have no conflicts of interest relevant to this article.

Acknowledgments

This study was financially supported by JSPS Grant-in-Aid for Scientific Research (JP19K19032, 17H06953 to H. Mitarai, 19H03832 to N. Wada).

References

1. Fletcher DA, Mullins RD. Cell mechanics and the cytoskeleton. *Nature* 2010;463:485—92.
2. Perrin BJ, Ervasti JM. The actin gene family: function follows isoform. *Cytoskeleton* 2010;67:630—4.
3. Desmoulière A, Redard M, Darby I, Gabbiani G. Apoptosis mediates the decrease in cellularity during the transition between granulation tissue and scar. *Am J Pathol* 1995;146:56—66.
4. Marconi GD, Fonticoli L, Rajan TS, et al. Transforming growth factor-beta1 and human gingival fibroblast-to-myofibroblast differentiation: molecular and morphological modifications. *Front Physiol* 2021;12:676512.
5. Hinz B, Celetta G, Tomasek JJ, Gabbiani G, Chaponnier C. Alpha-smooth muscle actin expression upregulates fibroblast contractile activity. *Mol Biol Cell* 2001;12:2730—41.
6. Rockey DC, Weymouth N, Shi Z. Smooth muscle α actin (Acta2) and myofibroblast function during hepatic wound healing. *PLoS One* 2013;8:e77166.
7. Lekic P, Rojas J, Birek C, Tenenbaum H, McCulloch CA. Phenotypic comparison of periodontal ligament cells in vivo and in vitro. *J Periodontal Res* 2001;36:71—9.
8. Fujii S, Maeda H, Tomokiyo A, et al. Effects of TGF-beta1 on the proliferation and differentiation of human periodontal ligament cells and a human periodontal ligament stem/progenitor cell line. *Cell Tissue Res* 2010;342:233—42.
9. Blobe GC, Schiemann WP, Lodish HF. Role of transforming growth factor beta in human disease. *N Engl J Med* 2000;342:1350—8.
10. Chin D, Boyle GM, Parsons PG, Coman WB. What is transforming growth factor-beta (TGF-beta)? *Br J Plast Surg* 2004;57:215—21.
11. O'Kane S, Ferguson MW. Transforming growth factor beta s and wound healing. *Int J Biochem Cell Biol* 1997;29:63—78.
12. Pepper MS. Transforming growth factor-beta: vasculogenesis, angiogenesis, and vessel wall integrity. *Cytokine Growth Factor Rev* 1997;8:21—43.
13. Janssens K, ten Dijke P, Janssens S, Van Hul W. Transforming growth factor-beta1 to the bone. *Endocr Rev* 2005;26:743—74.
14. Massagué J. TGF-beta signal transduction. *Annu Rev Biochem* 1998;67:753—91.
15. Abdollah S, Macías-Silva M, Tsukazaki T, Hayashi H, Attisano L, Wrana JL. TbetaRI phosphorylation of Smad2 on Ser465 and Ser467 is required for Smad2-Smad4 complex formation and signaling. *J Biol Chem* 1997;272:27678—85.
16. Feng XH, Derynck R. Specificity and versatility in tgf-beta signaling through Smads. *Annu Rev Cell Dev Biol* 2005;21:659—93.
17. Hasegawa D, Wada N, Maeda H, et al. Wnt5a induces collagen production by human periodontal ligament cells through TGFbeta1-mediated upregulation of periostin expression. *J Cell Physiol* 2015;230:2647—60.
18. Wada N, Maeda H, Tanabe K, et al. Periodontal ligament cells secrete the factor that inhibits osteoclastic differentiation and function: the factor is osteoprotegerin/osteoclastogenesis inhibitory factor. *J Periodontal Res* 2001;36:56—63.
19. Hasegawa D, Wada N, Yoshida S, et al. Wnt5a suppresses osteoblastic differentiation of human periodontal ligament stem cell-like cells via Ror2/JNK signaling. *J Cell Physiol* 2018;233:1752—62.
20. Mitarai H, Wada N, Hasegawa D, et al. Transgelin mediates transforming growth factor-beta1-induced proliferation of human periodontal ligament cells. *J Periodontal Res* 2017;52:984—93.
21. Moon MY, Kim HJ, Kim MJ, et al. Rap1 regulates hepatic stellate cell migration through the modulation of RhoA activity in response to TGF-β1. *Int J Mol Med* 2019;44:491—502.
22. Bergers G, Song S. The role of pericytes in blood-vessel formation and maintenance. *Neuro Oncol* 2005;7:452—64.
23. Dorotheou D, Bochaton-Piallat ML, Giannopoulou C, Kiliaridis S. Expression of α-smooth muscle actin in the periodontal ligament during post-emergent tooth eruption. *J Int Med Res* 2018;46:2423—35.
24. Norris RA, Damon B, Mironov V, et al. Periostin regulates collagen fibrillogenesis and the biomechanical properties of connective tissues. *J Cell Biochem* 2007;101:695—711.
25. Sawada T. Ultrastructural localization of fibrillin-1 and fibrillin-2 in oxytalan fibers in periodontal ligament of Japanese Macaca fuscata monkey. *J Mol Histol* 2010;41:225—31.
26. Silverio-Ruiz KG, Martinez AE, Garlet GP, et al. Opposite effects of bFGF and TGF-beta on collagen metabolism by human periodontal ligament fibroblasts. *Cytokine* 2007;39:130—7.
27. Smith PC, Martínez C, Martínez J, McCulloch CA. Role of fibroblast populations in periodontal wound healing and tissue remodeling. *Front Physiol* 2019;10:270.
28. Petrov VV, Fagard RH, Lijnen PJ. Stimulation of collagen production by transforming growth factor-beta1 during differentiation of cardiac fibroblasts to myofibroblasts. *Hypertension* 2002;39:258—63.
29. Olson EN, Nordheim A. Linking actin dynamics and gene transcription to drive cellular motile functions. *Nat Rev Mol Cell Biol* 2010;11:353—65.
30. Haase K, Al-Rekabi Z, Pelling AE. Mechanical cues direct focal adhesion dynamics. *Prog Mol Biol Transl Sci* 2014;126:103—34.
31. Drummond ML, Li M, Tarapore E, et al. Actin polymerization controls cilia-mediated signaling. *J Cell Biol* 2018;217:3255—66.

32. Qin Z, Fisher GJ, Voorhees JJ, Quan T. Actin cytoskeleton assembly regulates collagen production via TGF-β type II receptor in human skin fibroblasts. *J Cell Mol Med* 2018;22:4085—96.
33. Hubchak SC, Runyan CE, Kreisberg JI, Schnaper HW. Cytoskeletal rearrangement and signal transduction in TGF-beta1-stimulated mesangial cell collagen accumulation. *J Am Soc Nephrol* 2003;14:1969—80.
34. Shi Z, Rockey DC. Upregulation of the actin cytoskeleton via myocardin leads to increased expression of type 1 collagen. *Lab Invest* 2017;97:1412—26.